Paper

Surge Simulation in Pulse Transformer Model by Numerical Electromagnetic Field Computation

Akira Fujita* Student Member
Shohei Kato* Member
Takao Hirai** Member
Shigemitsu Okabe** Member

In this paper we present transient analysis of transformer models by the moment method in frequency domain. The results show that the secondary voltage has the peak which is higher than the voltage calculated by the primary voltage and the winding ratio. The inductance of the winding and the capacitance between windings have an influence on a surge in the transformer winding. In addition to the transient analysis we calculate the inductance from time responses and the impedance in low frequency, and compare them with the analytical equation which is based on Nagaoka factor.

Keywords: moment method, inductance, capacitance, surge, transformer winding

1. Introduction

In electric power system a threat of a lighting surge is decreased by using ground wires and arresters, but the risk of the failure of transformers is still high. A transformer winding is the most familiar conductor configuration of electromagnetic field components such as the transformer, resistors, reactance devices and etc. Therefore, it is important that we investigate the lighting surge how to advance into the winding. When we simulate a surge in the transformer, because the electromagnetic coupling at each part of winding is inhomogeneous, it is required to make an equivalent circuit which is different from the general transmission and the distribution circuit in surge analysis.

Recently many equivalent circuits are used for surge simulation in a transformer, but there is the problem that the electric potential distribution is not determined only the inductance. Capacitance affects surge dominantly in the high frequency domain. And exact surge analysis has many difficult things [1]~[4]. Then, we previously simulate surge characteristic by numerical electromagnetic field computation from the geometric and material data without equivalent circuit [7]~[12]. These results clarify an electric potential and electric field distribution of an air-core coil in time domain, the increase of the rise time as a result of the large inductance and the extension of the period of the damped oscillation in a single phase transformer with an iron-core. This paper presents surge simulations in transformer models by numerical field computation in frequency domain, and converts to time domain by inverse Fourier transform.

* Toyo University
2100, Kujirai, Kawagoe 350-8585
** Tokyo Electric Power Company
4-1, Egasaki, Tsurumi-ku, Yokohama 230-8510

2. Simulation Method and Models

To calculate the electromagnetic field in a magnetic and a dielectric substance by numerical computation method, there are two kinds of moment method; time domain method and frequency domain method. We use the moment method in frequency domain because an easy handling of 3-dimensional structure and a good stability of numerical computation. The moment method based on NEC-2 [14] is adopted. In this paper conductors are simulated by the perfect conductors and thin wire approximation, and the iron-core is approximated by cubic cells in the method of equivalent magnetomotive force [15] to calculate the electric and magnetic flux.

Fig. 1(a) shows the air-core transformer model. The diameter of the conductor is 1 mm, the rectangular section is 120 mm × 150 mm, and the number of the turns of the winding is 100. The secondary winding is formed by 10 turns of 126 mm × 56 mm × 15 mm. The voltage source locates in the central part of the rectangular from the coil 40 mm away, and applies a step of 1 kV to the primary coil through the source resistance of 1 kΩ. Fig. 1(b) shows the iron-core transformer model inserted the iron-core into the air-core transformer. The iron-core has specific permeability 90, conductivity 1.0 S/m and the size of 118 mm × 48 mm × 160 mm. The voltage source is also 1 kV by step function as well as the air-core model. Because the inductance becomes larger by the iron-core, we set the source resistance to 10 kΩ for asymptotic to a stationary value in simulation time. Fig. 1(c) shows the iron-core transformer model with the closed magnetic circuit. The core size is 120 mm × 170 mm × 266 mm, and has a hollow of 120 mm × 74 mm × 170 mm. In this case also, the winding is the same as the air-core transformer model of Fig. 1(a). The voltage source and the source resistance are the same case shown in Fig. 1(b).

Simulation conditions are the following: the frequencies are from 0.2 MHz to 25.6 MHz with the increment step of 0.2 MHz for the air-core model and opened iron-core model, and from 0.05 MHz to 6.4 MHz with the incremental step of 0.05 MHz for the closed iron-core model. The segment length of the conductor is 0.05 m and the number of segments is 1112. The iron-core is simulated by the 1020 cubic cells of $9.8 \times 9.6 \times 9.4$ mm in the opened iron-core transformer model, and 1536 cells of $14 \times 15 \times 12$ mm in the closed one. They take computing time with 100 minutes in the air-core transformer model, 8 hours in opened iron-core model, and 19 hours in closed iron-core model secondary open-circuited by a personal computer with Pentium4 2 GHz processor.

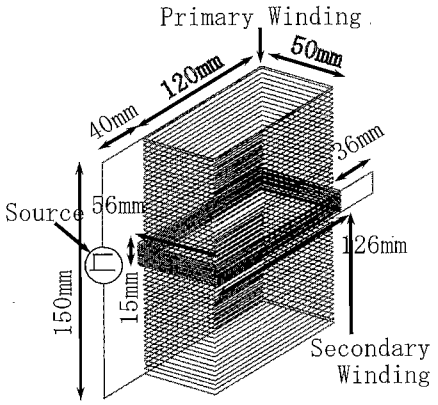

(a) Air-core transformer model

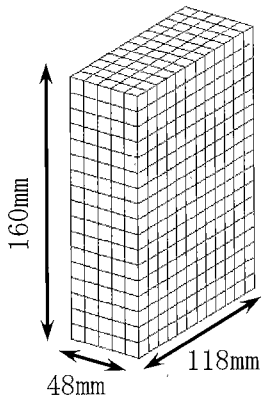

(b) Iron core transformer model
(Magnetic circuit is opened)

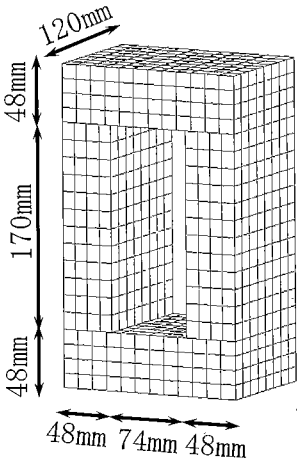

(c) Iron core transformer model
(Magnetic circuit is closed)

Fig. 1. Simulation models

3. Simulation Result

3.1 Air-core Transformer Model

3.1.1 Short-circuited secondary Fig. 2 shows time dependencies of the voltage and current in the primary circuit when the secondary is short-circuited. The voltage has the peak of 0.90 kV at about 60 ns, and at the same time a small peak appears in the rising phase of current characteristic. We can also find the damped oscillation that is caused by the leakage reactance in the primary and the electrostatic coupling between the windings. The time constant of current is about 439 ns and the inductance is calculated to 0.439 mH by the time constant and the source resistance 1 kΩ. In addition, we also calculate the inductance from the input impedance of the primary coil at 1 kHz, and the value is 0.425 mH.

The secondary current is shown in Fig. 3. The time dependency is almost the same as the primary current shown in Fig. 2. However, the asymptotic values are different. The current ratio is to 1 : 2.8 and differs from the relationship of the winding ratio in a case of an ideal transformer.

3.1.2 Open-circuited secondary The Voltage and current in the primary circuit are shown in Fig. 4 when the secondary is open-circuited. We find a voltage peak of 0.94 kV and the current shows a small peak

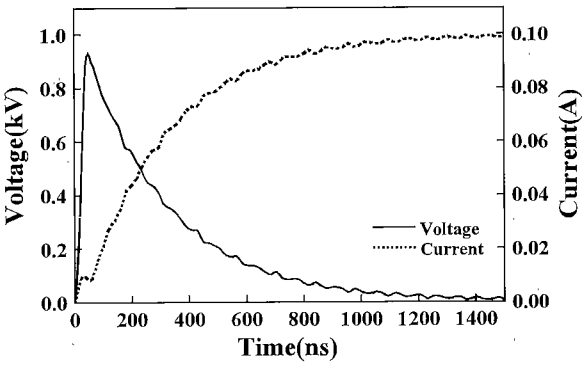

Fig. 2. Primary voltage and current when secondary is short-circuited of air-core transformer model

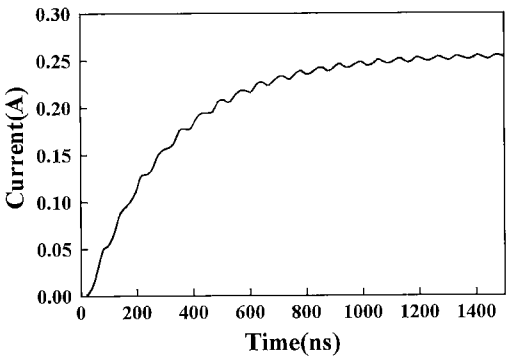

Fig. 3. Secondary current when the secondary is short-circuited of air-core transformer model

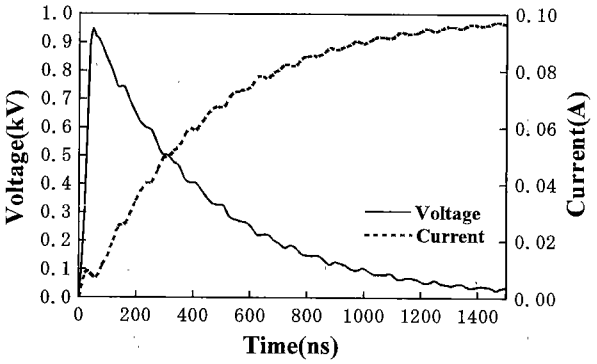

Fig. 4. Primary voltage and current when secondary is open-circuited of air-core transformer model

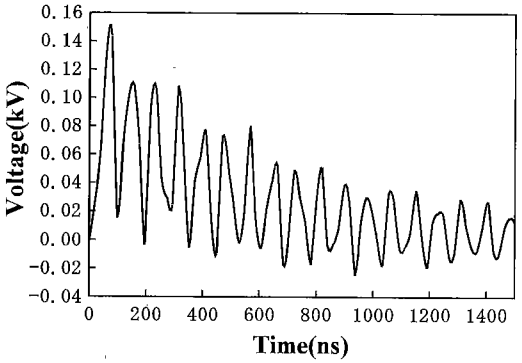

Fig. 5. Secondary voltage when the secondary is open-circuited of air-core transformer model

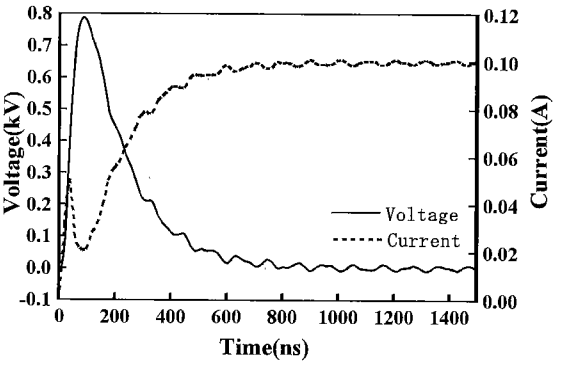

Fig. 6. Primary voltage and current when secondary is short-circuited of opened iron-core transformer model

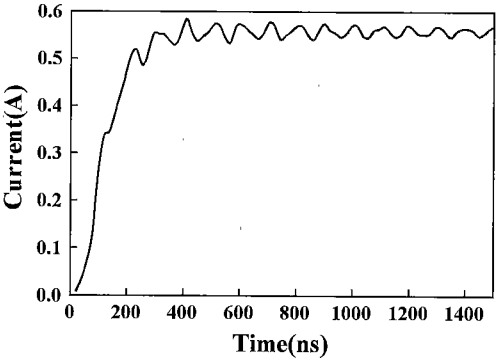

Fig. 7. Secondary current when the secondary is short-circuited of opened iron-core transformer model

of 0.09 A at the same time. Moreover when comparing Fig. 2 and Fig. 4, the wave tail of the voltage in open-circuited is prolonged, and also the rise time of the current increases. As well as the short circuited, the leakage reactance in the primary and the electrostatic coupling between the windings lead to the damped oscillation. At the open circuited secondary, the time constant of current is 440 ns and the source resistance is 1 kΩ, therefore, the inductance is calculated to 0.44 mH. We can also obtain the inductance 0.412 mH from the analytical equation based on the Nagaoka factor. In addition, we also calculate the inductance from the input impedance of the primary coil at 20 kHz and the value becomes 0.414 mH.

The secondary voltage when the secondary is open-circuited is shown in Fig. 5. The maximum voltage is about 0.15 kV. This value is lager than the value calculated by the winding ratio 10 : 1 and the primary voltage shown in Fig. 4 using the assumption of the ideal transformer. The secondary voltage shows a damped oscillation of which the period is about 80 ns and this oscillation resembles the primary one. This means that the resonant phenomenon is caused by the leakage reactance in the primary and the electrostatic coupling between the windings.

3.2 Opened Iron-core Transformer Model

3.2.1 Short-circuited secondary Fig. 6 shows the voltage and current when the secondary is short-circuited in the opened iron-core transformer model and Fig. 7 shows the secondary current. In Fig. 6 the peak of voltage is about 0.78 kV. It is noted that the source resistance is 10 kΩ which is ten times of the air-core transformer model. The time dependencies of the voltage and the current in Fig. 6 are almost the same as in Fig. 4, except the following points. The first is a prominent peak at the rising phase of the current, and we can find the damped oscillation which is brought about by the leakage reactance in the primary and the electrostatic coupling between the windings. The oscillation period is longer than the air-core transformer model. The second is larger time constant of the voltage and current. By the insertion of the iron-core to the air-core transformer model, the inductance increases and results the larger time constant of both the voltage and current, and the longer oscillation period. Because the leakage magnetic flux decreases, the current ratio increases to 1 : 5.5. The inductance is estimated at 2.3 mH because the time constant of current is 234 ns and the source resistance is 10 kΩ. We also calculate the inductance from the input impedance of the primary coil at 20 kHz and the value becomes 2.1 mH. The small peak of the current may be due to the capacitance between coils and the iron-core because the current builds up slowly if the inductance plays an important role in the difference.

3.2.2 Open-circuited secondary The primary circuit voltage and current at the secondary shorted circuit are shown in Fig. 8. Comparing the results of short-circuited secondary shown in Fig. 2, the rise time

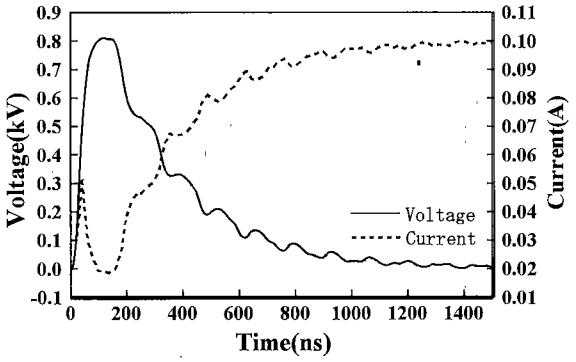

Fig. 8. Primary voltage and current when secondary is open-circuited of opened iron-core transformer model

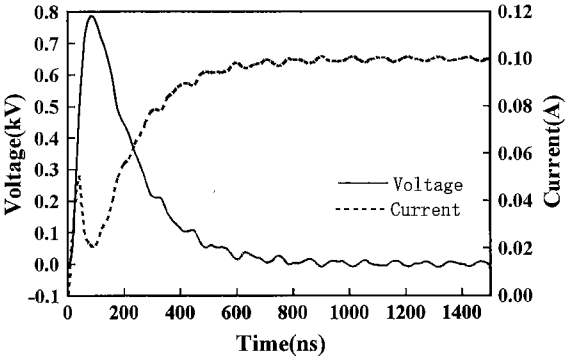

Fig. 10. Primary voltage and current when secondary is short-circuited of closed iron-core transformer model

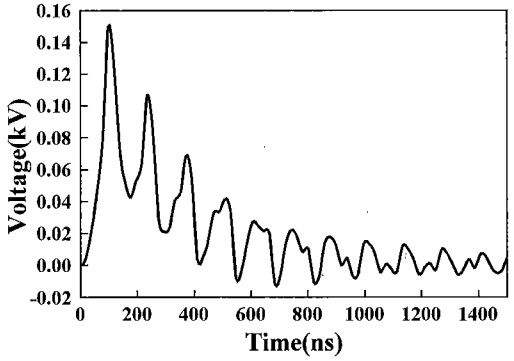

Fig. 9. Secondary voltage when the secondary is open-circuited of opened iron-core transformer model

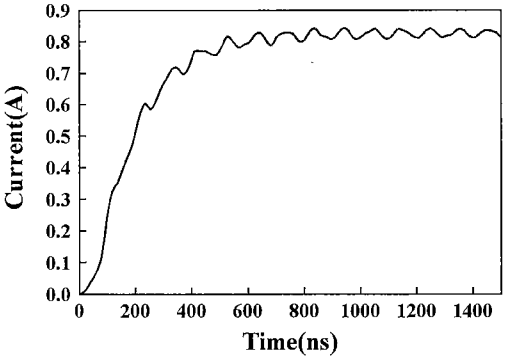

Fig. 11. Secondary current when the secondary is short-circuited of closed iron-core transformer model

of current and the peak of voltage increase slightly. The damped oscillation takes place by the leakage reactance in the primary and the electrostatic coupling between the winding, as well as short circuited. However the period is larger than the short circuited because the inductance of the exciting reactance is in series with the primary circuit without the secondary leakage reactance in parallel with the exciting circuit at the short-circuited secondary.

The time constant of current is 320 ns and the inductance is calculated to 3.2 mH by the time constant and the source resistance 10 kΩ. We calculate the input impedance of the primary coil at 20 kHz and the inductance is 3.0 mH.

Fig. 9 shows the voltage at the secondary opened circuited. The secondary voltage also shows the damped oscillation of which period is about 130 ns. The period is lager than the air-core transformer model shown in Fig. 5. This is caused of the increase of the inductance and the capacitance of the coils. As well as the air-core transformer, the oscillation period of the secondary voltage is similar to the primary.

3.3 Closed Iron-core Transformer Model

3.3.1 Short-circuited secondary Fig. 10 shows the primary voltage and current when secondary is short-circuited. The primary voltage has 0.79 kV peak. Because of the closed magnetic circuit, the magnetization impedance increases and also the peak voltage increases. The damped oscillation appears and the oscillation period is longer than the air-core transformer model and the opened iron-core transformer model. Because the leakage magnetic flux decreases in the closed iron-core model and the current in the secondary circuit increases, the current ratio increases to about 1 : 8.0. This relation is larger than the air-core and the opened iron-core transformer model. Finding the time constant from the primary circuit voltage, we can get the inductance 2.4 mH. The inductance is also calculated to 2.2 mH by the input impedance at 20 kHz. The inductance is also higher than the opened iron-core model.

3.3.2 Open-circuited secondary The time dependencies of the voltage and current in the primary circuit are shown in Fig. 12 when the secondary is open-circuited. We can see the peak voltage and the rising time lager than the secondary short-circuited. The damped oscillation is not prominent, and this shows that the energy loss in the primary circuit becomes large. At the open-circuited secondary, the exciting circuit is connected in a series in the primary circuit, and the exciting loss may be larger than the other model because of the larger volume of the iron-core.

The voltage at the secondary opened circuit is shown in Fig. 13. Fig. 13 also shows the damped oscillation whose period is almost the same as the period in the opened iron-core model. This oscillation is caused by the reflection of surge between the primary circuit winding ends, the resonance of the leakage reactance and the electrostatic coupling between the windings. The

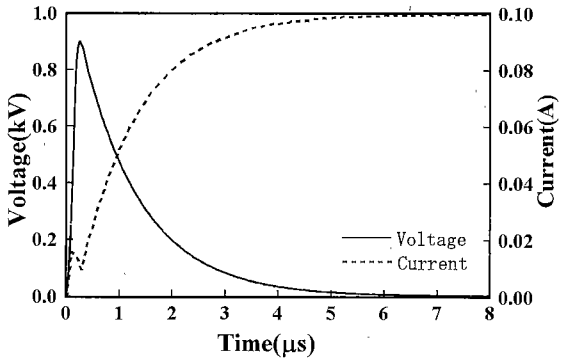

Fig. 12. Primary voltage and current when secondary is open-circuited of closed iron-core transformer model

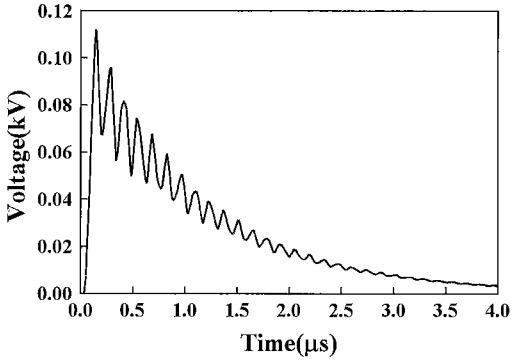

Fig. 13. Secondary voltage when the secondary is open-circuited of closed iron-core transformer model

time constant of the current is 1.3 μs and the inductance is calculated to 13.0 mH by the time constant and the source resistance 10 kΩ. As the other method, we can obtain the inductance from the following analytical equation of the magnetic circuit.

$$L = \mu_r \mu_0 \frac{S}{\ell} N^2 \quad \cdots\cdots\cdots\cdots\cdots\cdots\cdots\cdots\cdots\cdots\cdots\cdots (1)$$

where S is the area of cross section of the iron core, ℓ is the length of the magnetic flux path, and N is the number of the turns of winding. The 10.3 mH is estimated from the above formula. In addition, the calculation of the input impedance of the primary coil at 20 kHz gives the inductance 11.1 mH.

4. Discussion

In the case of the air-core transformer model, the primary voltage and current show almost the same time dependencies in spite of the secondary circuit condition as shown in Fig. 2 and Fig. 4. From this result, it is considered that the leakage reactance is large. Generally, an air-core coil has the smaller magnetizing reactance and larger leakage reactance than an iron-core one. Therefore, the ratio of the magnetizing current to the primary current increases and the current ratio is smaller than the winding ratio. The voltage ratio is also smaller than the winding ratio because of the voltage drop of the leakage reactance in the non-ideal transformer. The simulation result, however, shows that the current ratio is

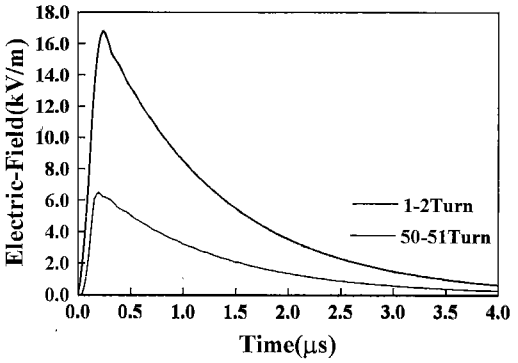

Fig. 14. Electric field in primary winding turns

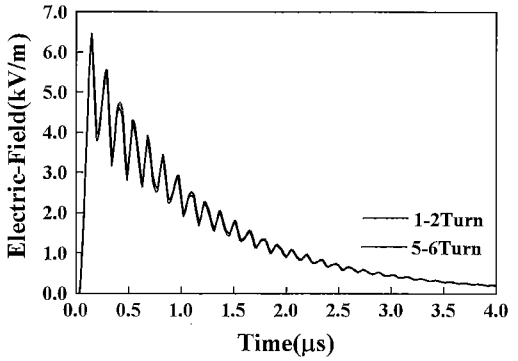

Fig. 15. Electric field in secondary winding turns

1 : 2.8 lower than the current estimated from the winding ratio, and on the other hand the voltage ratio is 1 : 0.15 higher. It is likely that the electrostatic coupling between the windings resonates with the leakage reactance and cause the voltage difference.

On the other hand, in the case of the iron-core transformer model, the difference of the shorted and the opened circuit is larger as shown in Fig. 6 and Fig. 8. The difference is more remarkable in the closed iron-core transformer model as shown in Fig. 10 and Fig. 12. This is caused by the increase of the magnetization impedance, when the iron-core is inserted into the coils.

In the simulation results, we mainly studied the time dependency of the voltage and current but an electric field between the turns and the layer is important to the dielectric design of a transformer. We simulated the electric field of an axis component at every 10th turn, when the applied voltage is 1 kV and the secondary is open circuited. Fig. 14 shows the axial component of the electric field between the first turn and the second turn, between the 50th turn and the 51th turn in the primary winding. In Fig. 14 we can find about 16.6 kV/m maximum peak at the end part of winding. However, the electric field at the central part of the winding is much smaller than the one at the terminal.

The axial component of the electric field between the first turn and the second turn, and the fifth turn and the sixth turn in the secondary winding are shown in Fig. 15 when we calculated the electric field per a turn at the same condition as Fig. 14. The peak of the electric field is about 6.46 kV/m at the end part, and the peak is almost the same value at the central part. Comparing

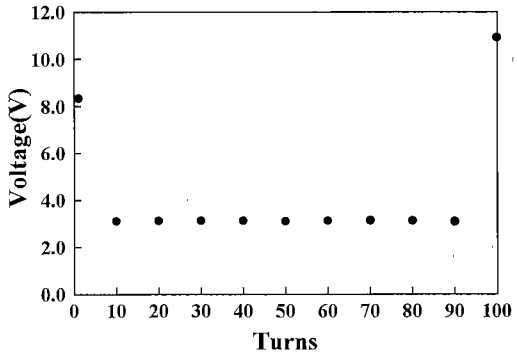

Fig. 16. Voltage distribution between primary winding turns

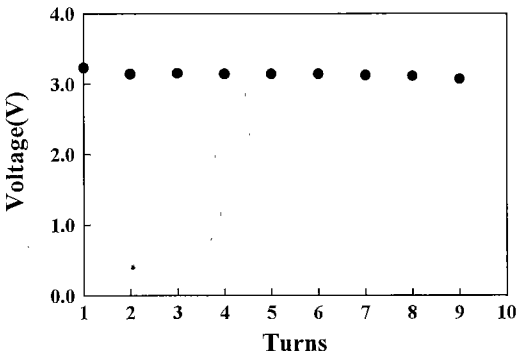

Fig. 17. Voltage distribution between secondary winding turns

the result shown in Fig. 14, the electric field in the secondary winding turn is smaller than the one in the primary winding turn. Two electric fields at 1–2 turn and 5–6 turn are almost the same because the secondary coil is located on the middle of the primary coil. The period of oscillation is similar to the secondary circuit voltage.

In addition to the electric field, we studied the voltage between winding by the product of the distance between turns and the axis component of the electric field between turns. Fig. 16 shows the voltage distribution between the primary winding, and Fig. 17 shows the voltage distribution between the secondary winding.

In Fig. 16 the voltage has the maximum at the end part, and shows a nearly symmetrical distribution to the center. However, in Fig. 17, the voltage distribution in the secondary winding is not symmetry, and the end part does not show the maximum. Comparing the results of the air-core coil model [11], the period of oscillation increases and the voltage between turns decreases. These results are caused by the magnetization impedance which increases when the iron-core is inserted into the winding.

In this paper we use specific permeability 90 such as ferrite for high frequency range, which is adapted in the pulse transformer. In generally, however, power transformers are made by silicon steel which specific permeability is several thousands. If at high specific permeability the skin depth becomes small, we may be required to make a fine volume mesh for the iron-core to keep the simulation accuracy.

Except the air-core model, the magnetic core makes a simulation model to be almost an ideal transformer because of the decrease of the leakage flux. However, the transient voltage and current do not have the relation of the primary and secondary which follows the ratio of windings. Therefore, it is necessary to construct an equivalent circuit of a transformer model which handles the electrostatic coupling between windings and a magnetic core.

Table 1. The inductance value of the transformer model

Model	Secondary Condition	Time Constant	Analytical Equation	Input Impedance
Air-core	Short	0.439	0.412	0.425
Transformer	Open	0.44	0.412	0.414
Opened Iron-Core	Short	2.3	/	2.1
Transformer	Open	3.2	3.1	3.0
Closed Iron-Core	Short	2.4	/	2.2
Transformer	Open	13.0	10.3	11.1

As it is important to investigate the accuracy of the simulation results, we check the accuracy comparing with the inductances calculated, and show them in Table 1. In the air-core model, we find close agreement among values calculated by the time constant of step response, the impedance at 1 kHz and the analytical formula with Nagaoka factor. We also compare the calculated inductance with the theory of the magnetic circuit in the closed iron-core model. The inductance calculated by the time constant is slightly higher than other two values. However, we obtain the close agreement between the inductance of the impedance method and that estimated by the theory of the magnetic circuit.

5. Conclusion

We calculated surge in the air-core transformer model, opened iron-core transformer model, and closed iron-core transformer model by moment method. The results show that the secondary voltage has the maximum which is higher than that estimated by the primary voltage and the winding ratio. Surge in transformer winding depends on not only the inductance of the winding but the capacitance among the windings and the iron-core. Comparing three inductances calculated from the time response, the impedance in low frequency and the analytical equation based on Nagaoaka factor to investigate the simulation accuracy, close agreement between them was obtained. It is proved that the simulation of transient electromagnetic phenomenon in transformer is possible by moment method.

To develop a moment method applicable to the dielectric design of high voltage power transformers, it is necessary to handle a high permeability and a multi layer structure in addition to large volume in geometrically.

(Manuscript received March 3, 2003,
revised July 8, 2003)

References

(1) T. Noda, H. Nakamoto, and S. Yokoyama: "A Simplified Model of Pole-Type Distribution Transformaer for Surge Calculations", 1998 National Convention, IEE Japan, p.1652 (1998) (in Japanese)

(2) K. Michishita, H. Takagi, and Y. Hongo: "Modeling of Pole-Type Distribution Transformer for Analysis of Lighting Surge on middle-VoltagePower Line", *T. IEE Japan*, Vol.119-B, No.10, pp.1128–1129 (1999-10) (in Japanese)

(3) T. Noda, H. Nakamoto, and S. Yokoyama: "A detailed Model of Pole-Type Distribution Transformaer for Surge Calculations", Proc. of 1998 Annual Conference of Power & Energy Society, IEE Japan, 375 (1998) (in Japanese)

(4) K. Iga, K. Michishita, and Y. Hongo: "Study of Equivalent Circuit of Pole-mounted Transformer for Analysis of Lighting Surge", Proc. of 2002 Annual Conference of Power & Energy Society, IEE Japan, No.470 (2002) (in Japanese)

(5) A.M. Miri, A.J. Schwab, and M.A. Nothaft: "High-Frequency Simulation of High-Voltage Transformer", 7th International High Voltage Symposium, pp.135–138 (1991)

(6) A.M. Miri and A.O. Hauser: "Improved FE-method for the Simulation of Behavior of System with Multi-turn Windings in the Case of Transient Excitations", 9th International High Voltage Symposium, No.8342 (1995)

(7) R. Elarbi, S. Kato, A. Mochizuki, and E. Zaima: "Transient Electric Field in Winding", 9th International High Voltage Symposium, No.8359 (1995)

(8) S. Kato: "Simulation of Surge on Transformer Winding by Numerical Electromagnetic Field Analysis", The Papers of Technical Meeting on Research Society Data of High Voltage, IEE Japan, HV-00-43 (2000)

(9) A. Fujita, S, Kato, T. Hirai, and S. Okabe: "Surge Simulation in Transformer Model by Numerical Electromagnetic Filed Computation", 2002 National Convention Record IEE Japan, No.7-167 (2002) (in Japanese)

(10) A. Fujita, S, Kato, T. Hirai, and S. Okabe: "Surge Simulation in Transformer Modelby Numerical Electromagnetic Filed Computation (PartII)", Proc. of 2002 Annual Conference of Power & Energy Society, IEE Japan, No.18-471 (2002) (in Japanese)

(11) A. Fujita, S, Kato, T. Hirai, and S. Okabe: "Transient Characteristic in Air Core Coil by Numerical Electromagnetic Field Computation", Proc. of 2002 Annual Conference of Fundamentals and Materials Society, IEE Japan, No.I-3 (2002) (in Japanese)

(12) A. Fujita, S, Kato, T. Hirai, and S. Okabe: "Surge Simulation in Transformer Model by Numerical Electromagnetic Field Computation", 3rd International Workshop on High Voltage Engineering, ED-03-35, SP-03-24, HV-03-24 (2003)

(13) A. Fujita, S, Kato, T. Hirai, and S. Okabe: "Transient Analysis of Air-Core Coils by Moment Method", IEEJ Trans., FM, Vol.123, No.2, pp.202–203 (2003-2) (in Japanese)

(14) G.J. Burke and A.J. Pogio: "Numerical Electro-magnetics Code-Method of Moment", NOSC TD 166, Vol.2, Lawrence Livermore Laboratory (1981)

(15) J.J.H. Wang: Generalized Moment Method in Electromagnetics, Wiley, New York (1991)

Akira Fujita (Student Member) He graduated from the Department of Electric and Electronics in the Faculty of Engineering at Toyo University in March 2002. Now he is a M.S. student in Toyo University, Japan.

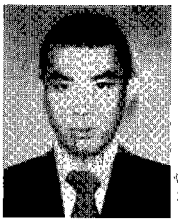

Shohei Kato (Member) He graduated from the Department of Electrical Engineering at Yokohama National University, March 1971. He received the Dr.Eng. Degree in Electrical Engineering from University of Tokyo, Japan in 1976. From April, he was lecturer in the Toyo University, and he is professor 1993. He engaged mainly in research related to measuring high voltage, Numerical computation, discharge phenomena, and lighting surge.

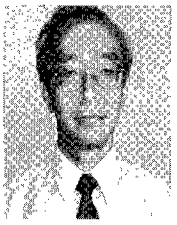

Takao Hirai (Member) He graduated from the Department of Electronics and Communications in the Faculty of Science and Engineering at Waseda University in March 1991. He entered Tokyo Electric Power Company in April of the same year. He engaged mainly in research related to lighting measurement and surge analysis in distribution systems.

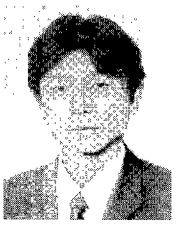

Shigemitsu Okabe (Member) He received the Dr.Eng. Degree in Electrical Engineering from University of Tokyo, Japan in 1986. From April, 1986 he joined Tokyo Electric Power Company. Dr. Okabe was a visiting researcher in the Munich Engneering University, Germany in 1992. Now, he is group Manager of the power Engneering R&D Center. He is a member of IEEE.